Chandra Observations of MBM-12: X-rays from the Local Bubble

Richard J. Edgar
Randall K. Smith, Peter E. Freeman, Paul Plucinsky, Beth Biller
Smithsonian Astrophysical Observatory

Abstract:

We present the results of a 100 ksec Chandra observation (obsid 943) of MBM 12, a nearby $[d >\sim 90pc, (l, b) = 159.1, -34.5)]$ molecular cloud. Snowden, McCammon & Verter (1993) used deep ROSAT PSPC observations of this cloud to measure the foreground 1/4 keV band emission from the Local Bubble. They also put strong upper limits on the foreground 0.5–1.0 keV (M-band) emission. Most, if not all, models for the Local Bubble predict that the emission in this bandpass is primarily due to O VII and O VIII lines. We report a detection with high statistical confidence of oxygen emission arising between the observer and this cloud. Many statistical and systematic effects are considered, including: low energy ACIS quantum efficiency and redistribution functions; charged particle backgrounds; statistical biases.

We acknowledge support from NASA contract NAS8–39073 with the Chandra X-ray Center, and Chandra guest observer grant GO0–1097X.

The Idea

- MBM 12 is a nearby dark cloud. *ROSAT* found (Snowden, McCammon & Verter 1993) a 3/4-keV flux consistent with zero, but a positive 1/4-keV flux.
- Models of the Soft X-ray Diffuse Background which produce the 1/4-keV band emission also produce O VII (561–574 eV) and O VIII lines (654 eV).
- We obtained a 100 ks observation of MBM 12, which was broken into two segments, to look for these Oxygen lines.
- Non x-ray background dominates the data; careful characterization of and removal or fitting of this background is challenging, as the source fills the field of view.
- We present results for the S3 chip here. I-array data are consistent (though with less statistical significance due to the lower QE), and S1 data await further analysis. The S1 chip is further from the center of the cloud, and so of less use.

Background Measurement & Modeling

- Non sky-looking background datasets have been obtained several times, by moving the Integrated Science Instrument Module to a position midway between the ACIS and HRC in-focus positions. This leaves ACIS looking only at the ISIM wall, away from the sky and the on-board calibration source.
- A small area of the HRC can be operated simultaneously, to obtain far off-axis images of the Chandra HRMA point spread function.
- We used obsids 4286 and 62850.
- Elevated background times were excluded from the analysis.
- Background data were processed in the same way as the on-source data.
- A function was fit to the spectrum from 0.35–5 keV, consisting of a Broken power law at low energies, and a few Gaussian fluorescent components. The 3 lines are Al K-α, Si K-α, and the Au M complex.

The MBM 12 Data

- A total of 100 ks of data were taken on MBM 12.
- The two observing intervals were separated by three weeks. Observation dates were 2000 July 10 and Aug 17.
- The charged particle background environment was higher during the first observing interval (obi0); it was very quiet during the second interval (obi1).
- Point sources (including XY Ari) were removed.
- Background rate flares were removed by excising intervals of time.
- PI (gain corrected) spectra were obtained for the whole S3 chip. Weighted response matrices (RMF) and ancillary response files (ARF) were obtained using CXC tools.
- The ARF files (effective area as a function of energy) were corrected for ACIS filter contamination using the `contamarf2` software available on the ACIS contributed software page.

Model Fitting

- The MBM 12 data were background subtracted. Backgrounds were scaled to reflect the differing rates for the two observing intervals. This cancelled the fluorescent lines seen in both the background and on-source data.
- An inspection of the background-subtracted spectra suggested a gain error of approximately 2% exists in the CXC response matrix for S3. Since similar effects have been seen in the calibration data (supernova remnant E0102; Raley, Edgar and Plucinsky, private communication), we adjusted the energies of the input model.
- Fluxes were corrected for the energy dependence of the ARF.
- Data from both observing intervals were jointly fit to the same model:
  - A redshifted APEC model without O VIII and O VII lines. This model component supplies the continuum and weak lines. The temperature was set to $kT = 0.114$ keV. Allowing this parameter to vary does not significantly change the results. The redshift was set to 2% to correct for the detector gain error.
  - Two Gaussians to represent the O VII triplet (0.568 keV) and O VIII Lyman–α line (0.653 keV). These lines were artificially moved 2% to the red to correct for the detector gain error.
- O VIII is detected with high confidence.
- Only an upper limit to the O VII was obtained.
- The best-fit intensity of the O VIII line is:

line	significance %	sigma	limit photons cm^{-2} s^{-1} sr^{-1}
O VII	+99.73	3	1.95
O VII	+90	1.6	1.05
O VII	+99	2.6	1.67
O VII	+95.45	2	1.29
O VII	+68.27	1	0.63
O VIII	+99.73	3	3.32
O VIII	+99	2.6	3.17
O VIII	+95.45	2	2.99
O VIII	+90	1.6	2.85
O VIII	+68.27	1	2.65
O VIII	**best fit**		2.36
O VIII	−68.27	−1	2.01
O VIII	−90	−1.6	1.81
O VIII	−95.45	−2	1.71
O VIII	−99	−2.6	1.51
O VIII	−99.73	−3	1.38

- Compare these numbers to the Gendreau et al (1995) ASCA all-sky diffuse background result of 2.3 ± 0.3 and 0.6 ± 0.15 photons $\mathrm{cm}^{-2}\ \mathrm{s}^{-1}\ \mathrm{sr}^{-1}$, for the O VII and O VIII lines, respectively.
- This suggests that any O VII emission arising beyond the cloud is shadowed by it, and that there is excess O VIII emission in this direction.
- We do **not** however, see the continuum reported by Gendreau et al. Perhaps whatever source contributes the continuum is shadowed by MBM 12, while the oxygen lines are not.
- This detection is about half the Snowden, McCammon, & Verter *ROSAT* upper limit in this direction.
- Solar Wind oxygen ions charge exchanging from the solar wind should produce a large O VII/O VIII ratio, and surface brightnesses of this order (depending on what part of the heliosphere one looks through).
- Note that a feature consistent with an O VII line appears only in the first OBI (top plots). Possible time-dependence of the heliospheric contribution may be implicated.

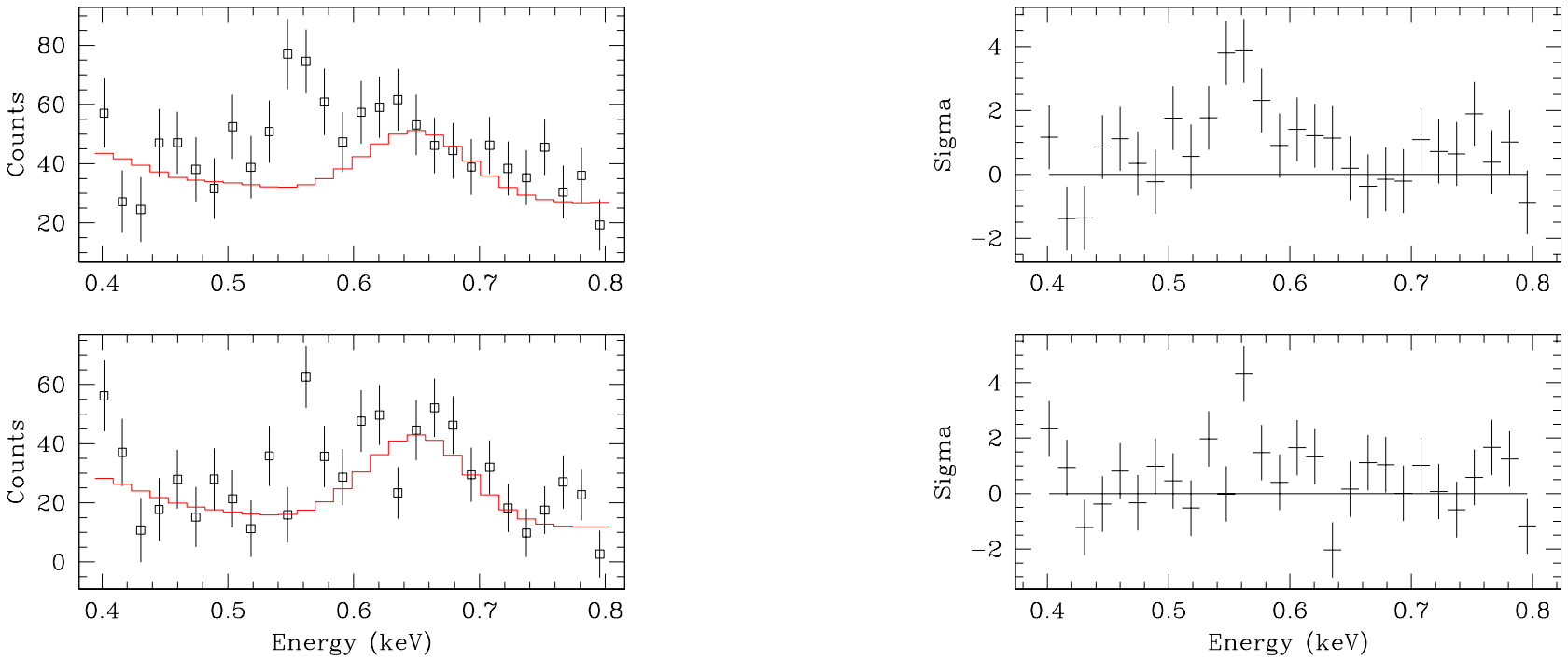

Figure 1: Left: Best joint fit of MBM-12 data (both observing intervals). Note the prominent O VIII line, and the excess near O VII in the top plots only. Top panel: OBI0. Bottom panel: OBI1. Right: Residuals from the fit.

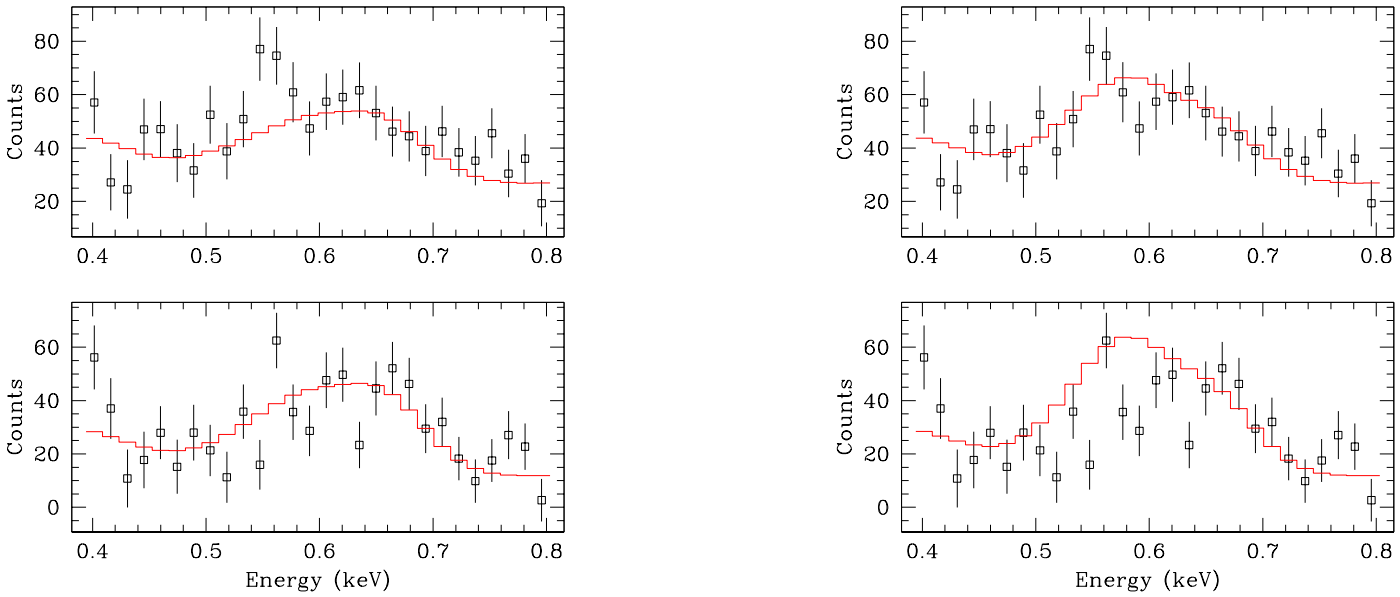

Figure 2: Fits from Figure 1 with an O VII line introduced. Left: equal strength Right: twice the O VIII line strength. Note that while the top (OBI0) data are better fit, the quality of the joint fits are degraded.

Conclusions

- There is an oxygen line in the diffuse x-ray background, even toward MBM-12, a nearby dark cloud.
- The large O VIII/O VII ratio is inconsistent with a heliospheric origin from charge exchange between interstellar neutrals and the highly charged oxygen in the solar wind.

Future Work

- Similar analyses can be carried out for most of the other chips (I array). The lower QE is compensated by better background rejection for these chips, so they will contribute a similar number of photons to the analysis. A first look at these data shows a consistent but not highly significant detection.
- Further scrutiny of the background, and methods for modeling and subtracting it. A more careful look at detector gains.
- Detailed modeling of the heliospheric charge exchange emission, including the time dependence of this effect.

REFERENCES

Gendreau, K. C. et al. 1995, PASJ, 47, L5.
Raley, M., Edgar, R. J., and Plucinsky, P. P. 2003 (private communication)
Snowden, S. L., McCammon, D., & Verter, F. 1993, ApJ, 409, L21.